Clim Dyn (2010) 35:331–340
DOI 10.1007/s00382-009-0664-y

New approach for optimal perturbation method in ensemble climate prediction with empirical singular vector

Jong-Seong Kug · Yoo-Geun Ham · Masahide Kimoto · Fei-Fei Jin · In-Sik Kang

Received: 28 November 2008 / Accepted: 9 September 2009 / Published online: 17 September 2009

Abstract In this study, a new method is developed to generate optimal perturbations in ensemble climate prediction. In this method, the optimal perturbation in initial conditions is the 1st leading singular vector, calculated from an empirical linear operator based on a historical model integration. To verify this concept, this method is applied to a hybrid coupled model. It is demonstrated that the 1st leading singular vector from the empirical linear operator, to a large extent, represents the fast-growing mode in the nonlinear integration. Therefore, the forecast skill with the optimal perturbations is improved over most lead times and regions. In particular, the improvement of the forecast skill is significant where the signal-to-noise ratio is small, indicating that the optimal perturbation method is effective when the initial uncertainty is large. Therefore, the new optimal perturbation method has the potential to improve current seasonal prediction with state-of-the-art coupled GCMs.

J.-S. Kug (✉)
Korea Ocean Research and Development Institute,
Ansan, Korea
e-mail: jskug@kordi.re.kr

Y.-G. Ham · I.-S. Kang
School of Earth and Environment Sciences,
Seoul National University, Seoul, Korea

M. Kimoto
Center for Climate System Research,
University of Tokyo, Tokyo, Japan

F.-F. Jin
Department of Meteorology, SOEST,
University of Hawaii, Hawaii, USA

Keywords Optimal perturbation method · Seasonal prediction · Ensemble prediction · Singular vector

1 Introduction

As scientific and economic interests in seasonal climate prediction and predictability have increased considerably in recent years, many studies have been devoted to its implementation and improvement. Since the seasonal prediction is basically an initial value problem in a Tier-1 prediction system, which use a coupled GCM containing an interactive physics between atmosphere and ocean (e.g. Kug et al. 2008), the initialization is an essential component for seasonal predictability. The initialization consists of two parts. The first is to make a best estimate, which indicates accurate and well-balanced initial conditions. The second is to make optimal initial perturbations, which shall represent the uncertainty of the estimate for the initial conditions. The former has been paid a great deal of attention by a number of studies. However, the latter still remains problematic. For example, the ensemble seasonal forecasts at operational centers still face the difficulty that the ensemble perturbations from a single coupled ocean–atmosphere model have limited growth at early forecast leads relative to the amplitude of mean error (Vialard et al. 2003; Palmer et al. 2004; Saha et al. 2006). This implies their initial perturbations may be not optimal. In this study, therefore, we focus on the optimal initial perturbations for ENSO forecasts.

It is certain that every initial condition contains initial uncertainty due to the imperfection of the estimate. That is, an initial uncertainty, due to errors in the initial conditions, is inevitable. This initial error grows as the model

is integrated, and it degrades the performance of the prediction. It is known that ensemble prediction can reduce a prediction error, originated from the initial uncertainty (Molteni and Palmer, 1993; Buizza et al. 1998). As the number of ensemble members is increased, the prediction error due to the initial uncertainty can be effectively reduced (Kumar and Hoerling 2000; Yoo and Kang 2005). However, with limited computing resources, it is important to know how to generate initial perturbations (i.e. initial ensemble spread) that effectively reduce initial uncertainty.

For this purpose, it is well known that a fast-growing mode can be an optimal perturbation for ensemble prediction. For example, Toth and Kalnay (1997) pointed out that the prediction error is greatly reduced when a pair of fast-growing perturbations is used for initial perturbation, since the average of a pair of ensembles filters out the fast-growing errors. This is because fast-growing errors dominate the total errors right after the start of prediction, while non-growing (or slow-growing) errors do not contribute much to the prediction errors.

To detect the fast growing modes, two methods are well known and commonly used. One is the singular vector method. This method was first proposed for weather forecasting at the European Centre for Medium-Range Weather Forecasts (ECMWF) (Farrell 1989; Mureau et al. 1993; Palmer et al. 1994; Molteni et al. 1996). Unstable perturbation patterns were calculated from the singular vectors of the linear propagator of the primitive equations. This method was also adopted to intermediate coupled models (Moore and Kleeman 1996, 1997a, b, 1998). The other technique, to obtain a fast growing mode, is the so-called breeding method (Toth and Kalnay 1993, 1997; Corazza et al. 2003). Toth and Kalnay (1993) firstly suggested the breeding method for the most fast-growing perturbation in a weather forecast system. After their first attempts, a few studies have applied bred vectors from seasonal to interannual time scales using an intermediate coupled model (Cai et al. 2003) and Coupled GCMs (Yang et al. 2006, 2008).

Although the two methods are well-suited for weather and extended weather forecasting, they have some limitations in seasonal predictions. In the breeding method, the rescaled pattern from the perturbed integration is again used for the initial perturbation of the next perturbed integration. Therefore, if the initial perturbation has a similar structure (i.e. spatial pattern) to the final perturbation, the initial perturbations, rescaled from the final perturbation, can grow as fast as a fast-growing perturbation does. It is valid when the fast-growing mode is stationary or propagating with a similar pattern. Otherwise, the growth of the perturbation can be slow down. In this view, the bred vector is appropriate for the extended weather forecast because the synoptic baroclinic eddies propagate eastward with a similar wave structure. However, the fast-growing modes of longer time scales have significant structural evolution over time. For example, the initial perturbation is somewhat different from the final perturbation in the fast growing mode of the tropical Pacific (See Fig. 2). The initial perturbation of the heat content shows zonally uniform pattern, indicating the recharge mode, while the final perturbation shows zonally asymmetric pattern, indicating sea-saw pattern. In this case, if the final perturbation is used as an initial perturbation, the growth of the perturbation can be slower down. This means the bred vector can be sometimes far from the fast-growing initial perturbation.

The singular vector method also has some difficulties in applying seasonal prediction. Firstly, this method requires a linearized version of a coupled model, which is the most difficult part. Also, the singular vector method extracts a fast-growing mode from the linearized operator. In this sense, it is somewhat problematic to capture modes associated with long-term timescale variability because the linearized system has a difficulty to capture a nonlinear behavior by short-term variation when the lead time is longer. In addition, they also required extra computer resources to generate initial perturbations as much as generating initial states.

Due to these limitations of applying the singular vector method in seasonal prediction, other alternative methods have been suggested to extract singular modes in a coupled system (Blumenthal 1991; Chen et al. 1997; Xue et al. 1997a, b), for example a linear Markov model (Blumenthal 1991), linear inverse model (Tziperman et al. 2008) and a perturbing forward linear model (Lorenz 1965; Xue et al. 1994, 1997a,b; Chen et al. 1997; Fan et al. 2000; Kleeman et al. 2003; Tang et al. 2006). Most of these studies applied their methods to ENSO simulation. They all revealed the dependency of optimal growth on the seasonal cycle and ENSO phase and discussed its implication for ENSO predictability. So far, however, they did not apply their singular vector methods to the ensemble prediction.

In this study, we have developed an empirical singular vector method to extract a fast-growing mode for the initialization of seasonal climate prediction. This method is quite similar to that of Blumenthal (1991). The fast-growing mode is captured by calculating a singular vector from an empirical operator. Using the empirical singular vector as an initial perturbation, the impact of the optimal perturbation is assessed in a hybrid coupled model. In Sect. 2, the hybrid coupled model is briefly described and the empirical singular vector method is introduced. Section 3 describes the results from the optimal perturbation methods. A brief summary and discussion are included in Sect. 4.

2 Model and methods

2.1 Hybrid coupled model

In this study, a hybrid coupled model is used to examine the optimal perturbation method. The oceanic component of the hybrid coupled model is based on an intermediate ocean model similar to the Cane-Zebiak (CZ) model (Zebiak and Cane 1987). The difference between the present ocean model and the original one is that it uses a new parameterization of subsurface temperature (Kang and Kug 2000). The atmospheric component of the hybrid model is SPEEDY AGCM (Simplified Parameterizations, primitivE-Equation DYnamics, Molteni 2003). The goal of this model is to achieve computational efficiency while maintaining characteristics similar to state-of-the-art AGCMs with complex physics. The resolution of the model is T42L10 (horizontal spectral truncation of 42 wave numbers and 10 vertical levels). Details on the coupled model and its performance are referred to Ham et al. (2009).

2.2 Empirical singular vector method

To extract a fast growing mode in the seasonal time scale, we developed an empirical singular vector method in this study. This method is based on the concept of Singular Vector Method (Farrell 1989; Palmer et al. 1994; Molteni et al. 1996), but it uses an empirical operator instead of a dynamical operator. The detailed description of this method is as follows;

Let us assume that nonlinear integration can be approximately expressed by a simple linear operator (L) of the evolution of the state vector from time η to time $\eta + \tau$ as follows:

$$Y_n = X_{n+\tau} = LX_n + \varepsilon \tag{1}$$

where X and Y are state vectors of the prediction model. The parameter, τ, is the lead time for model integration. In seasonal prediction, X and Y can be regarded as the initial condition and the prediction with lead time, τ, respectively. The variable, ε, denotes error from the linear approximation. In the conventional singular vector method, the linear operator, L, is calculated by linearizing the governing equation of the prediction model. However, it is also possible to estimate the operator empirically from the historical data. If there are historical data from the long-term model integration, the linear operator can be calculated as follows:

$$L = YX^T(XX^T)^{-1} \tag{2}$$

This formula is basically the same as the linear inverse modeling approach (e.g. Blumenthal 1991; Moore and Kleeman 2001; Penland 1996; Penland and Matrosova 1998, 2001; Penland and Sardeshmukh 1995; Penland et al. 2000; Tziperman et al. 2008). By solving singular values of the linear operator, L, the singular vectors can be calculated.

$$u_i Y = s_i v_i X \tag{3}$$

where s_i, u_i, and v_i are the ith singular value and its corresponding singular vectors, respectively. If the singular value, s_i, is greater than one, it implies that the singular mode grows in the linear operator. Also, the fast growing mode of the linear operator is consistent with the singular mode, which has a maximum singular value. Therefore, the singular vector can be the optimal perturbation in an ensemble seasonal prediction.

2.3 Applying ESV method to the hybrid coupled model

In order to apply the ESV to prediction of the hybrid model, the linear operator is obtained in a reduced space through EOF analysis. For the initial state vector, X in Eq. 1, the EOF analysis is applied to the instantaneous thermocline depth data from 100-year long simulation. In this study, only the first 5 modes are used to estimate the linear operator, but our major results are not sensitive to the number of the EOF mode. The 5 dominant EOF modes explain over 80% of total variance of thermocline depth. Because most memories for ENSO prediction reside in the thermocline depth, only the thermocline depth is adopted to represent initial perturbations in ESV. For the prediction state, Y in Eq. 1, the EOF analysis is also applied to the monthly mean SST data from the same 100-year long simulation. Also, the first 5 modes are used in this study. The 5 dominant EOF modes explain over 90% of the total variance of SST. Because our major target is SST prediction associated with ENSO, the first ESV mode should capture the optimal perturbation for SST growing. Therefore, we use only SST variables as the prediction state vector(Y). However, the variables of the prediction state can be changed according to the target of the prediction. For example, if the main target of the prediction is for the Indian Ocean, we can select the proper initial and final prediction variables in constructing the linear operator.

Based on the principal components of the EOF modes, the linear operator (L) is estimated. Note that we use 6-months as the lead time, τ, in order to capture a slowly-varying mode associated with ENSO which has a nearly 4-year time scale in the model. Therefore, the linear operator is constructed based on 6-month lag relation between thermocline depth and SST. In addition, because the pattern of the fast-growing mode depends on the seasonal cycle, the EOF analysis is applied for each month of the calendar year, and thus the linear operator is separately calculated for each month. From the estimated linear

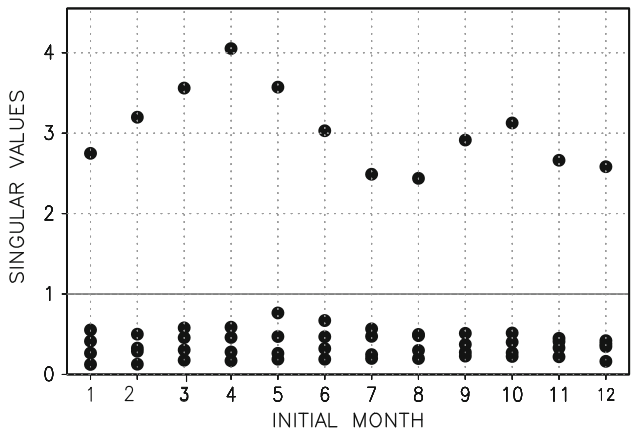

Fig. 1 Singular values at each calendar month from empirical Singular Vector method

operator, five singular modes are extracted. Among them, the mode, having the largest singular value, is selected as an optimal perturbation mode. Figure 1 shows the singular values for each month. In most seasons, there is only one growing singular mode, whose singular value is greater than one. Note that the singular value starting from April (August) shows the largest (smallest) value.

Figure 2 shows an example of the first leading singular mode for the case starting from April, whose singular value is the largest. Though we only used thermocline depth (SST) data for the initial (final) state, the pattern for the other variables is also calculated by a linear regression. The initial state of the thermocline shows a deepened thermocline over the whole equatorial region and shoaling in the off-equatorial region, though the detailed zonal distribution are somewhat different. These patterns are quite similar to the recharge pattern of the equatorial heat content in the Recharge Oscillator (Jin 1996, 1997a, b), indicating El Nino development. According to this initial state, the singular mode shows a large SST anomaly 6-months later over the eastern Pacific. This feature is quite similar to the singular mode of Xue et al. (1997, see their Fig. 3). We found that the overall features of fast-growing modes in other seasons are also similar to those in Fig. 2.

2.4 Experimental prediction designs

Using the hybrid coupled model, an experimental ENSO forecast is performed. This experimental forecast is performed in the perfect model context, indicating that one realization of the coupled model is regarded as a true state. To make the initial conditions, the Ensemble Kalman Filter (EnKF, Evensen 1994, 2003; Leeuwenburgh 2007) is applied with 16 ensemble members. This experiment is identical to that of Ham et al. (2009). They carried out a 12-month lead ensemble forecast during a 20-year period, starting from initial conditions produced by EnKF analysis. Since 16-ensemble member is used for the EnKF analysis, 16-ensemble predictions are available. To compare the forecast skills of prediction with ESV perturbations, the averaged forecast skill of all possible combinations of two

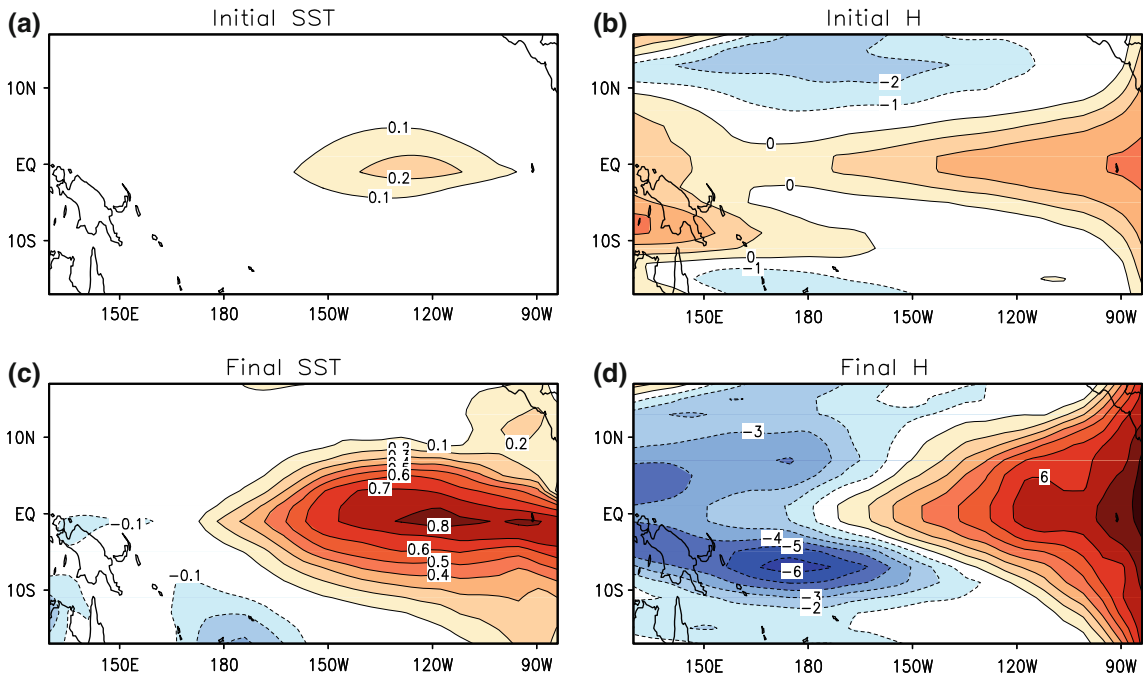

Fig. 2 First leading singular mode of (**a**) SST, and (**b**) thermocline depth in April, and final perturbation pattern of (**c**) SST, and (**d**) thermocline depth at September

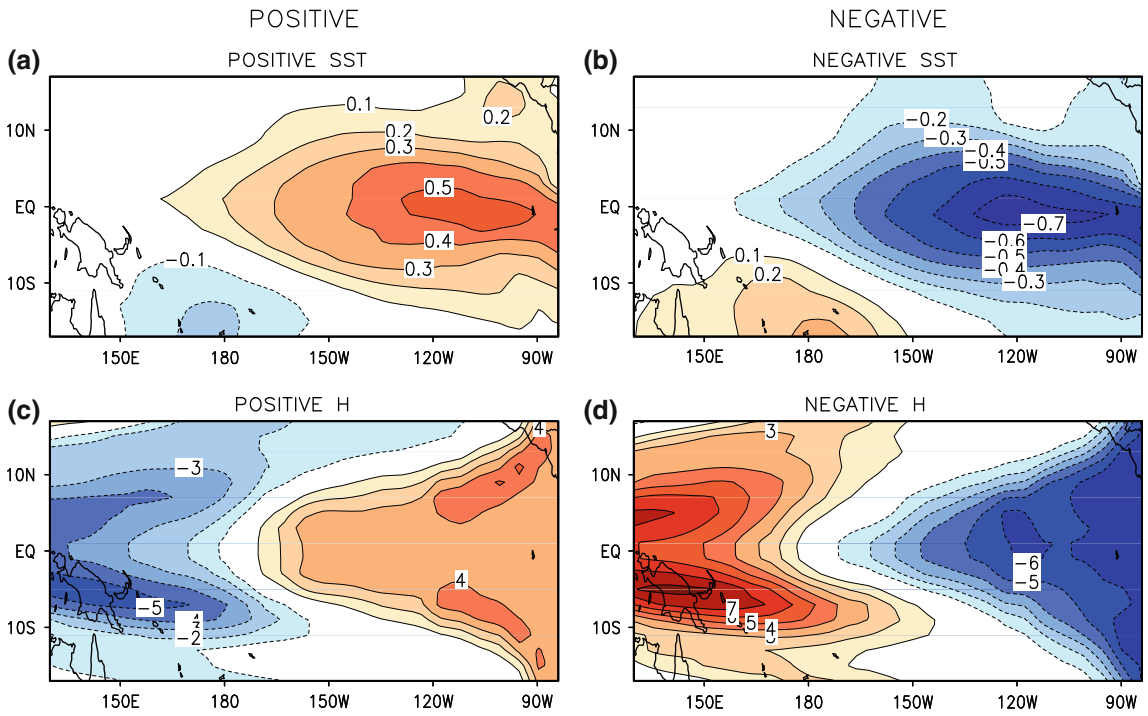

Fig. 3 Positive and negative perturbation patterns at 6-month lead forecast

ensemble members among 16 ensemble members (a total of 120 cases) is computed. This skill represents the mean correlation skill of the ensemble mean of two members. Hereafter, we will denote this forecast as the "CNTL prediction". The detailed procedures on initialization and prediction are referred to in Ham et al. (2009).

Based on the first leading singular mode, initial perturbations are generated. Because this singular mode only includes thermocline depth, perturbations for other variables in the atmosphere and ocean are calculated by regressing a time series associated with the singular vector of the thermocline. By adding and subtracting the perturbation to the ensemble mean state of 16 analysis values (initial conditions), a pair of initial conditions is generated. Using the initial conditions, a 12-month lead forecast is carried out. We will refer to this prediction as "ESV". The ESV prediction is compared to the CNTL prediction.

3 Results

Using the initial conditions with the optimal perturbations, a 12-month lead prediction is performed starting from each month of the 20-year period. Prior to comparing forecast skills, we examined how well the first singular vector captures the growth of the initial perturbation in the nonlinear integration. To do so, a final perturbation is calculated for positive and negative initial perturbations, respectively. The final pattern for the positive (negative) is calculated by averaging the difference between the 6-month lead forecast of the ensemble mean of CNTL and ESV with only positive (negative) perturbation members for the 20-year prediction. Figure 3 shows the final perturbation pattern from the prediction. It is clear that the patterns of the thermocline and SST are quite similar to the singular vectors, as shown in Fig. 2c, d. This indicates that the leading singular mode, calculated from the empirical linear operator, captures the growth of the initial perturbation in the nonlinear prediction well.

As shown in Fig. 1, the singular value of the leading mode strongly depends on the season. This indicates that the error growth, estimated from the empirical linear operator, strongly depends on seasonal factors. To estimate whether the nonlinear model also simulates the seasonal dependency of the error growth, we define an error growth rate from the prediction results. The definition is as follows:

$$\lambda_{\text{nonlinear}} = \frac{\int\int v_1 \cdot SST(t=6)\mathrm{d}x\mathrm{d}y}{\int\int u_1 \cdot H(t=0)\mathrm{d}x\mathrm{d}y}$$

where u_1, v_1 indicate singular vectors in Eq. 3. H is the thermocline depth at the initial condition and the SST is predicted SST at a 6-month lead in the EOF space. The basic formula of the error growth rate is the same as the definition of the singular value in Eq. 4.

Figure 4 shows the error growth rates as a function of seasonal cycle, measured from prediction results, and the

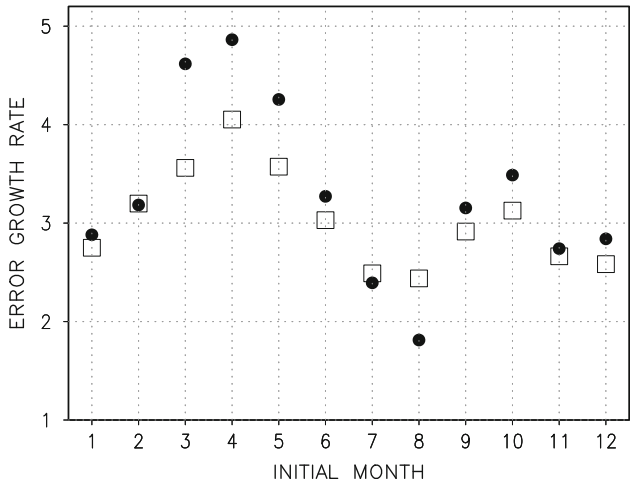

Fig. 4 Error growth rates as a function of seasonal cycle measured from prediction results (*enclosed circle*) and first leading singular value from empirical SV method (*open square*)

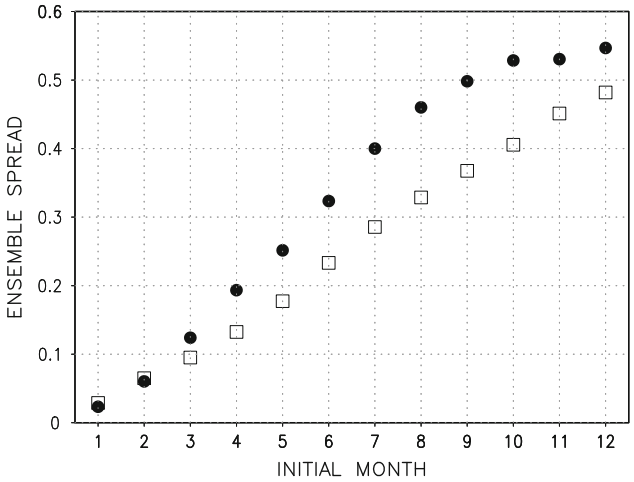

Fig. 5 Ensemble spread of NINO3 SST in the CNTL (*open square*), and ESV prediction (*enclosed circle*)

first leading singular value, from the empirical SV method. The error growth measured from the prediction results is largest in April and smallest during the boreal summer time. It is clear that this seasonal dependency is consistent with that of the first leading singular value. For example, the maximum and minimum phases of the leading singular value are mostly consistent with those of the error growth. Also, they both show a secondary maximum value during the boreal autumn time. Therefore, it seems that the present empirical linear operator, to a large extent, captures the leading mode of the nonlinear integration and its error growth.

Because we use the fast-growing perturbation, the initial perturbation will grow very rapidly as the prediction starts. Therefore, it is expected that the ensemble spread of the ESV will be larger than other initial perturbations. Figure 5 shows the ensemble spread of NINO3 SST in the CNTL and ESV prediction. To compare with the ESV prediction, the averaged ensemble spread of all the possible combinations of two ensemble members among the 16 ensemble members (total of 120 cases) is computed. The small initial spread grows rapidly as the prediction starts in both predictions. However, the spread of the ESV is larger than that of the CNTL over all month lead times. In particular, the spread difference is distinctive in 6–10 month lead forecasts. At a 6-month lead forecast, the spread of the ESV is 40% larger than that of the CNTL. This supports the view that the perturbation from the leading singular vector grows faster than those from CNTL.

In order to evaluate the role of the optimal initial perturbation, the forecast skill is compared between the CNTL and ESV predictions. This skill represents the correlation skill of an ensemble mean of two members. The correlation skill and RMS errors are used to evaluate the performance of the seasonal forecasts, as shown in Fig. 6. The ESV prediction has a better skill than the CNTL prediction over all forecast lead times. To confirm whether this improvement is significant, prediction skills with possible combinations of two ensemble members among the 16 ensemble members (total of 120 cases) are computed, and their distribution is constructed. Among 120 correlation values, 6th highest and lowest correlation values are drawn as 95% significant lines. The similar process is done for 99% significant lines. Based on the distribution, a statistical confidence level for the correlation (or RMSE) difference is calculated as shown in Fig. 6. It is clear that the forecast skill improvement of ESV prediction is significant, because ESV prediction skill is out of range of 99% significance level (dashed line). In particular, the forecast skill improvement is distinctive for long-lead forecasts. The correlation improvement increases as the lead time becomes longer, and the difference is almost saturated after a 6-month lead. These results support the view that the optimal initial perturbation can improve the prediction skill even on a seasonal time scale. Also, we found that the ESV prediction with two ensemble members has a comparable skill with that of the CNTL with 8 ensemble members (not shown), indicating that the optimal perturbation method is an effective way to represent the initial uncertainty with relatively few ensemble members. The RMSE also show consistent results, as shown in Fig. 6b.

Figure 7 shows the spatial patterns of correlation skill and RMS error of the CNTL prediction for SST anomalies (contour). It also shows the difference between the control and the ESV prediction (shading). Note that a positive sign denotes that the forecast skills of the ESV prediction are improved. The correlation skill of the CNTL is relatively low in the equatorial western Pacific compared to those in the off-equatorial eastern Pacific at 3- and 6-month lead

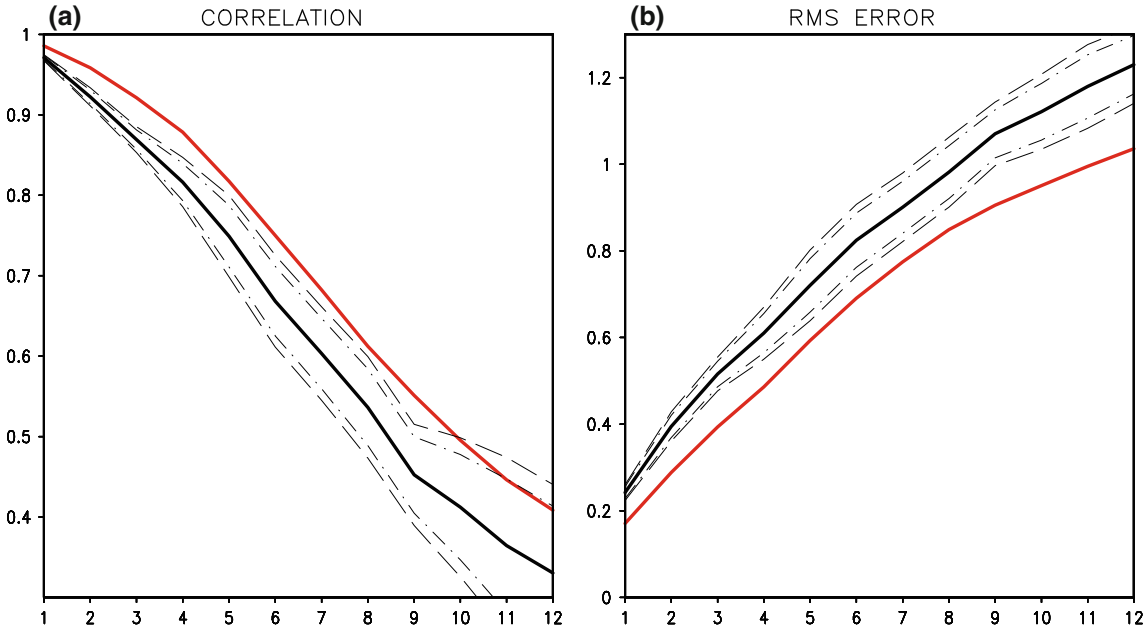

Fig. 6 (**a**) Correlation, and (**b**) RMS errors NINO3 SST anomalies in the CNTL (*black solid line*), and ESV prediction (*red solid line*). *Dashed and dashed-dotted lines* denote 99 and 95% confidence level, respectively

forecasts. It is clear that the ESV has higher correlation and lower RMS error over most regions and most lead times. However, the magnitude of the improvement depends on region and lead time. For example, the improvement in correlation and RMSE is more significant as the lead time becomes longer. It is also noted that that the improvement in correlation skill is robust over the region where the correlation skill is relatively low. In particular, the improvements of forecast skill are significant in the equatorial western Pacific compared to that in the off-equatorial eastern Pacific at 3 and 6-month lead forecasts. This implies that the effectiveness of the optimal perturbation method is related to the predictability.

In order to examine the relation further, signal to noise (STN) ratio is introduced in this study. The STN ratio is defined as follows (Rowell, 1998; Kang and Shukla 2006).

$$\text{Ratio} = \frac{\sigma^2_{\text{signal}}}{\sigma^2_{\text{noise}}} \tag{4}$$

where,

$$\sigma^2_{\text{signal}} = \frac{1}{N-1}\sum_{i=1}^{N}\left(\overline{x_i} - \overline{\overline{x}}\right)^2$$

$$\sigma^2_{\text{noise}} = \frac{1}{N(n-1)}\sum_{i=1}^{N}\sum_{j=1}^{n}\left(x_{ij} - \overline{x_i}\right)^2$$

The subscript i indicates the individual prediction, $N = 240$ (20 years $\times$ 12 months), j denotes the ensemble member, and $n = 16$. $\overline{\overline{x}}, \overline{x_i}$ are the climatology of ensemble mean and the ensemble mean, respectively. The STN is calculated from a CNTL prediction with 16 ensemble members. This definition is the same as that of Ham et al. (2009). Basically, larger (smaller) signal-to-noise ratio indicates higher (lower) predictability. Because the present prediction is done in the perfect model context, the STN ratio is directly related to the correlation skill of ensemble prediction when the number of ensemble members is large enough.[1]

To show the relationship between the correlation improvement and signal-to-noise ratio, a scatter diagram over the area 150°E–90°W, 10°S–10°N at 6-month lead forecast is shown in Fig. 8. It is clear that the correlation improvement is inversely proportional to the STN ratio. The inverse relationship is robust at 6–9 forecast lead months, but the relationship is also observed at other forecast lead months (not shown). These results are quite consistent with those of Ham et al. (2009).

Note that there is no model uncertainty in the perfect model context, so the signal-to-noise ratio (predictability) completely depends on the growth of the initial error. Namely, a smaller STN ratio indicates less predictability due to the large initial error growth. It is interesting that the STN ratio is closely related to the improvement of the ESV method. This means optimal perturbation works more effectively over the unpredictable region where the initial error growth is fast.

[1] The STN ration can be expressed by correlation coefficient (r) as follows: $\text{STN} = r^2/(1-r^2)$.

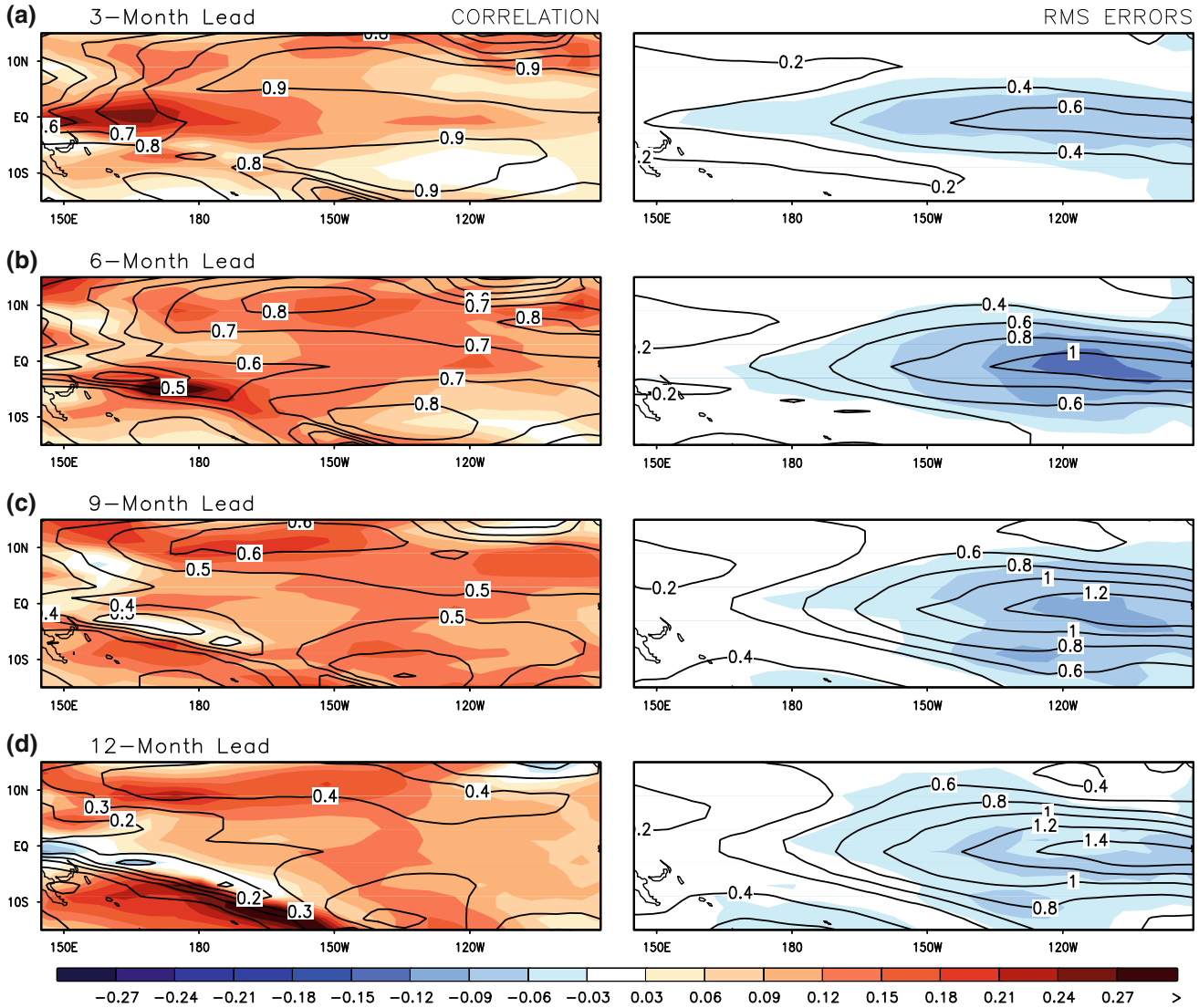

Fig. 7 Spatial pattern of (**a**) correlation, and (**b**) RMS errors for SST anomalies in the CNTL prediction (*contour*), and forecast skill improvements (*shading*). Note that *positive sign* denotes that forecast skills of the selected prediction are improved. The interval of shading is 0.03. *Red (blue) shading* indicates positive (negative) value

4 Summary and discussion

In this study, a new optimal perturbation method, the ESV method, has been developed to apply ensemble climate predictions. This method is to extract a fast growing mode based on an empirical linear operator. To test the idea, the ESV method is applied to 12-month lead ENSO prediction with a hybrid coupled model. First, we showed that the leading singular mode of the empirical linear operator is consistent with the fast-growing perturbation in nonlinear model predictions. It was also shown that the ESV had a significantly higher skill compared to that of CNTL. In addition, we found that the present optimal perturbation method is more effective over the unpredicted region due to the fast error growth of the initial error.

The present method has several benefits compared to the conventional methods, which are as follows. Firstly, it is very easy to extract the fast-growing modes by the present method. Without any numerical operation such as linearization of the model, the optimal perturbation can be easily obtained from a reduced EOF space. Thus, this method is applicable to any climate prediction model if their historical data are available. Second, it is flexible in selecting the norm and lead time dependent on prediction target. In this sense, it is useful for climate prediction because we can extract a fast growing mode in low-frequency motion, avoiding the high-frequency growing modes such as convective and baroclinic instabilities. Third, it does not require extra model integrations or computations to get the optimal perturbation. Thus, this

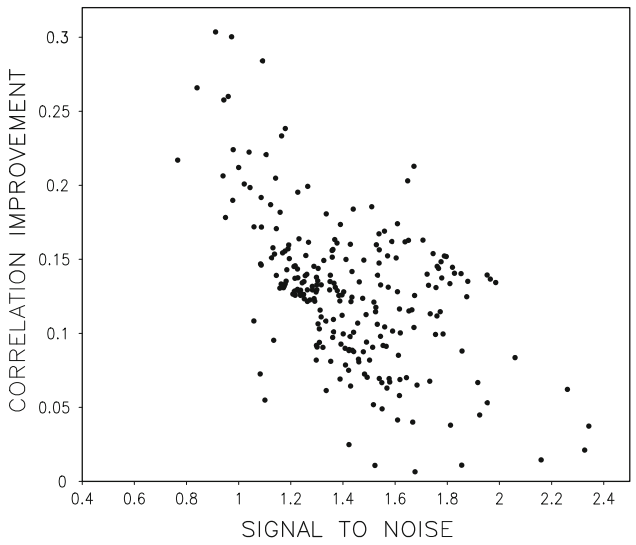

Fig. 8 Scatter diagram between correlation improvement (*y*-axis) and signal to noise ratio (*x*-axis) at 6-month lead forecast over eastern Pacific regions (150°E–90°W, 10°S–10°N)

method is computationally efficient compared to the other methods.

On the other hand, the present fast growing modes from the empirical linear operator are somewhat different from those of the conventional optimal perturbation method. The conventional breeding method and singular vector method try to extract a fast growing mode under time-dependent flow. These are close to Lyapunov vectors (Szunyogh et al. 1997; Toth and Kalnay 1997; Kalnay et al. 2002). However, the present method captures a fast growing mode under climatological flow of each calendar month. Thus, it is possible that the present empirical singular vector is sometimes different from the pattern of actual fast-growing error mode. Therefore, this method will be more effective when the pattern of the fast-growing mode is not very flow-dependent. It is still controversy that Xue et al. (1997a) showed that the dependency of the fast-growing mode on the ENSO phase is relatively smaller than its seasonal dependency, while Moore and Kleeman (1997a, b) showed a marked sensitivity of singular vectors to the phase of the ENSO cycle. Therefore, the degree to which fast growing modes are flow-dependent should be investigated further.

In this study, the ESV method is applied to the ENSO prediction of a hybrid coupled model to test new idea. The present results show that this method is of potential application to seasonal prediction of the complexity coupled GCM. In fact, our preliminary results with coupled GCMs reveal that the present method improve seasonal prediction of a coupled GCM (not shown). Further studies should be followed in this line. So far, most seasonal predictions of operations and research institutes did not use an optimal perturbation method to generate ensemble members. For instance, in two major experimental climate prediction projects of DEMETER (Palmer et al. 2004) and CliPAS (Wang et al. 2008), ensemble members are generated using the lagged method or using different atmospheric initial conditions. Presumably, this is because of the difficulty of applying the conventional optimal perturbation method. If our method works in a coupled GCM, it will give a chance to improve current state-of-art seasonal prediction.

Acknowledgments This work was mostly done when J.-S. Kug visited CCSR during the summer in 2007. J.-S. Kug is partly supported by KORDI(PE98425, PP00720, PM55290). F.-F. Jin was partly supported by NSF grants ATM-0652145 and ATM-0650552 and NOAA grants GC01-229. M. Kimoto was supported by Innovative Program of Climate Change Projection for the 21st Century of the Ministry of Education, Culture, Sports, Science and Technology of Japan.

References

Blumenthal MB (1991) Predictability of a coupled ocean–atmosphere model. J Clim 4:766–784

Buizza R, Petroliagis T, Palmer TN, Hamrud M, Hollingsworth A, Simmons A, Wedi N (1998) Impact of model resolution and ensemble size on the performance of an ensemble prediction system. Quart J R Meteor Soc 124:1935–1960

Cai M, Kalnay E, Toth Z (2003) Bred vectors of the Zebiak-Cane model and their potential application to ENSO predictions. J Clim 16:40–56

Chen Y-Q, Battisti DS, Palmer TN, Barsugli J, Sarachik ES (1997) A study of the predictability of Tropical Pacific SST in a coupled atmosphere–ocean model using singular vector analysis: the role of the annual cycle and the ENSO cycle. Mon Weather Rev 125:831–845

Corazza M, Kalnay E, Patil DJ, Yang S-C, Morss R, Cai M, Szunyogh I, Hunt BR, Yorke JA (2003) Use of the breeding technique to estimate the structure of the analysis "errors of the day". Nonlinear Process Geophys 10:1–11

Evensen G (1994) Sequential data assimilation with a nonlinear quasi-geostrophic model using Monte Carlo methods to forecast error statistics. J Geophys Res 99:10143–10162

Evensen G (2003) The Ensemble Kalman Filter: theoretical formulation and practical implementation. Ocean Dyn 53:343–367

Fan Y, Allen MR, Anderson DLT, Balmaseda MA (2000) How predictability depends on the nature of uncertainty in initial conditions in a coupled model of ENSO. J Clim 13:3298–3313

Farrell BF (1989) Optimal excitation of baroclinic waves. J Atmos Sci 46:1193–1206

Ham Y-G, Kug J-S, Kang I-S (2009) Optimal initial perturbations for El Nino ensemble prediction with Ensemble Kalman Filter. Clim Dyn. doi:10.1007/s00382-009-0582

Jin F-F (1996) Tropical ocean–atmosphere interaction, the Pacific Cold Tongue, and the El Niño-southern oscillation. Science 274:76–78

Jin F-F (1997a) An Equatorial Ocean recharge paradigm for ENSO. Part I: conceptual model. J Atmos Sci 54:811–829

Jin F-F (1997b) An Equatorial Ocean recharge paradigm for ENSO. Part II: a stripped-down coupled model. J Atmos Sci 54:830–847

Kalnay E, Corazza M, Cai M (2002) Are bred vectors the same as lyapunov vectors? AMS symposium on observations, data assimilation and probabilistic prediction, 13–17 January 2002, Orlando, Florida, pp 173–177

Kang I-S, Kug J–S (2000) An El-Nino prediction system using an intermediate ocean and a statistical atmosphere. Geophys Res Lett 15:1167–1170

Kang I-S, Shukla J (2006) Dynamic seasonal prediction and predictability of the monsoon, The Asian Monsoon, Springer/Praxis, Chapter 15

Kleeman R, Tang Y, Moore AM (2003) The calculation of climatically relevant singular vectors in the presense of weather noise as applied to the ENSO problem. J Atmos Sci 60:2856–2868

Kug J-S, Kang I-S, Choi D-H (2008) Seasonal climate predictability with tier-one and tier-two prediction systems. Clim Dyn 31. doi:10.1007/s00382-007-0264-7

Kumar A, Hoerling M (2000) Analysis of a conceptual model of seasonal climate variability and implications for seasonal prediction. Bull Am Meteorol Soc 81:255–264

Leeuwenburgh O (2007) Validation of an EnKF system for OGCM initialization assimilating temperature, salinity, and surface height measurements. Mon Weather Rev 126:125–139

Lorenz EN (1965) A study of the predictability of a 28-variable atmospheric model. Tellus 17:321–333

Molteni F (2003) Atmospheric simulations using a GCM with simplified physical parameterizations. I: model climatology and variability in multi-decadal experiments. Clim Dyn 20:175–191

Molteni F, Palmer TN (1993) Predictability and finite time instability of the northern winter circulation. Quart J R Meteorol Soc 119:269–298

Molteni F, Buizza R, Palmer TN, Petroliagis T (1996) The ECMWF ensemble prediction system: methodology and validation. Quart J R Meteorol Soc 122:73–119

Moore AM, Kleeman R (1996) The dynamics of error growth and predictability in a coupled model of ENSO. Quart J R Meteorol Soc 122:1405–1446

Moore AM, Kleeman R (1997a) The singular vectors of a coupled ocean–atmosphere model of ENSO I: thermodynamics, energetic and error growth. Quart J R Meteorol Soc 123:953–981

Moore AM, Kleeman R (1997b) The singular vectors of a coupled ocean–atmosphere model of ENSO II: thermodynamics, energetic and error growth. Quart J R Meteorol Soc 123:953–981

Moore AM, Kleeman R (1998) Skill assessment for ENSO using ensemble prediction. Quart J R Meteorol Soc 124:557–584

Moore AM, Kleeman R (2001) The differences between the optimal perturbations of coupled models of ENSO. J Clim 14:138–163

Mureau R, Molteni F, Palmer TN (1993) Ensemble prediction using dynamically conditioned perturbations. Quart J R Meteorol Soc 119:299–323

Palmer TN, Buizza R, Molteni E, Chen Y-Q, Corti S (1994) Singular vectors and the predictability of weather and climate. Philos Trans R Soc Lond 348:459–475

Palmer TN et al (2004) Development of a European Multimodel Ensemble System for seasonal-to-interannual prediction (DEMETER). Bull Am Meteorol Soc 85:853–872

Penland C (1996) A stochastic model of IndoPacific sea surface temperature anomalies. Phys D 96:534–558

Penland C, Matrosova L (1998) Prediction of tropical Atlantic Sea surface temperatures using linear inverse modeling. J Clim 11:483–496

Penland C, Matrosova L (2001) Expected and actual errors of linear inverse model forecasts. Mon Weather Rev 129:1740–1745

Penland C, Sardeshmukh PD (1995) The optimal growth of tropical sea surface temperature anomalies. J Clim 8:1999–2024

Penland C, Matrosova L, Weickmann K, Smith C (2000) Forecast of tropical SSTs using linear inverse modeling (LIM). Experimental Long-Lead Forecast Bulletin, Center for Ocean-Land–Atmosphere Studies 9:34–37

Rowell DP (1998) Accessing potential seasonal predictability with an ensemble of multidecadal GCM simulations. J Clim 11:109–120

Saha S et al (2006) The NCEP Climate Forecast System. J Clim 19:3483–3517

Szunyogh I, Kalnay E, Toth Z (1997) A comparison of Lyapunov and optimal vectors in a low-resolution GCM. Tellus A 49:200–227

Tang Y, Kleeman R, Miller S (2006) ENSO predictability of a fully coupled GCM model using singular vector analysis. J Clim 19:3361–3377

Toth Z, Kalnay E (1993) Ensemble forecasting and NMC: the generation of perturbations. Bull Am Meteorol Soc 74:2317–2330

Toth Z, Kalnay E (1997) Ensemble forecasting at NCEP and the breeding method. Mon Weather Rev 125:3297–3318

Tziperman E, Zanna L, Penland C (2008) Nonnormal thermohaline circulation dynamics in a coupled ocean–atmosphere GCM. J Phys Oceanogr 38:588–604

Vialard J, Vitart F, Balmaseda MA, Stockdale TN, Anderson DL (2003) An ensemble generation method for seasonal forecasting with an ocean–atmosphere coupled model. ECMWF Tech Memo 417:20

Wang B, Lee J-Y, Kang I-S, Shukla J, Kug J-S, Kumar A, Schemm J, Luo J-J, Yamagata T, Park C-K (2008) How accurately do coupled models predict the Asian–Australian Monsoon interannual variability? Clim Dyn 30. doi:10.1007/s00382-007-0310-5

Xue Y, Cane MA, Zebiak SE, Blumenthal B (1994) On the prediction of ENSO: a study with a low-order Markov model. Tellus 46A:512–528

Xue Y, Cane MA, Zebiak SE (1997a) Predictability of a coupled model of ENSO using singular vector analysis. PartI: optimal growth in seasonal background and ENSO cycles. Mon Weather Rev 125:2043–2056

Xue Y, Cane MA, Zebiak SE (1997b) Predictability of a coupled model of ENSO using singular vector analysis. PartII: optimal growth and forecast skill. Mon Weather Rev 125:2057–2073

Yang S-C, Cai M, Kalnay E, Rienecker M, Yuan G, Toth Z (2006) ENSO bred vectors in coupled ocean–atmosphere general circulation models. J Clim 19:1422–1436

Yang SC, Kalnay E, Cai M, Rienecker MM (2008) Bred vectors and tropical pacific forecast errors in the NASA coupled general circulation model. Mon Weather Rev 136:1305–1326

Yoo JH, Kang I-S (2005) Theoretical examination of a multi-model composite for seasonal prediction. Geophys Res Lett 32:L18707. doi:10.1029/2005GL023513

Zebiak SE, Cane MA (1987) A model for El Nino–southern oscillation. Mon Weather Rev 115:2262–2278